Tellus (1991), *43AB*, 82–103

Ocean circulation and climate change

By KLAUS HASSELMANN, *Max-Planck-Institut für Meteorologie, Bundesstrasse 55, D-2000 Hamburg 13, Germany*

(Manuscript received 4 September 1990; in final form 13 March 1991)

ABSTRACT

Recent numerical simulations using global ocean circulation models are reviewed together with model experiments involving further important climate sub-systems with which the ocean interacts: the atmosphere, the air-sea interface and the global carbon cycle. A common feature of all ocean circulation experiments considered is the strong sensitivity of the circulation to relatively minor changes in surface forcing, particularly to the buoyancy fluxes in regions of deep water formation in high latitudes. This may explain some of the well-known deficiencies of past global ocean circulation simulations. The strong sensitivity may also have been the cause of rapid climate changes observed in paleoclimatic records and can lead further to significant natural climate variability on the time scales of a few hundred years through the stochastic forcing of the ocean by atmospheric weather variability. Gobal warming computations using two different coupled ocean-atmosphere models for the "business-as-usual" scenario of the Intergovernmental Panel on Climate Change yield a significantly stronger warming delay due to the heat uptake by the oceans in the Southern Ocean than estimated on the basis of box-diffusion models. Recent advances in surface wave modelling, illustrated by a comparison of wave height fields derived from the WAM model and the GEOSAT altimeter, hold promise for the development of an improved representation of ocean-atmosphere coupling based on an explicit description of the dynamical processes at the air-sea interface. Global carbon cycle simulations with a three dimensional carbon cycle model tuned to reproduce past variations of carbon cycle indices show a significant impact of variations in the ocean circulation on the CO_2 concentration in the atmosphere and thereby on climate. The series of experiments suggest that for the study of climate in the time scale range from 10^{-1}–10^3 years, it would be highly desirable, and has indeed now become feasible, to couple existing, verified, climate sub-system models together in a comprehensive fully interactive model including the oceans, sea-ice, atmosphere, surface interface and the global carbon cycle.

1. Introduction

In the time-scale range from a few weeks to a thousand years, the dynamics of climate (defined here in the modern sense to encompass all time scales beyond the theoretical limits of deterministic weather prediction) is strongly controlled by the ocean. The atmosphere can be regarded on these time scales as in quasi-equilibrium. Since it responds to and acts back on changes in the ocean quasi-instantaneously, its time evolution need not be computed explicitly. Within the coupled ocean-atmosphere system it can therefore be treated formally as a diagnostic feedback loop with some superimposed white noise forcing. The ocean, however, must be modelled as a fully prognostic system, as it is the internal interactions within the ocean which largely govern the dynamical properties of the coupled ocean-atmosphere system, determining, for example, the transient response of the system to externally imposed forcing or natural climate variability.

Unfortunately, it has not yet been possible in practice to devise realistic models of the quasi-equilibrium statistically steady state of the atmosphere for given boundary conditions without actually integrating the full time-dependent equations of the nonlinear atmospheric circulation. The coupled ocean-atmosphere system can therefore be studied quantitatively in the time-scale range of interest only with coupled prognostic models of both the oceanic and the atmospheric circulation.

Even with present super-computers, however, finite computer resources limit such simulations to integration periods of the order of 100 years. Studies over longer time scales have therefore necessarily been qualitative and depend on the construction of some simplified diagnostic model of the atmospheric response and white noise atmospheric forcing.

In addition to the physical ocean-atmosphere circulation system, the dynamics of climate in the 10^{-1}–10^{3} year time-scale range is determined also by the cryosphere, carbon cycle, biosphere and geochemical cycles. I shall restrict myself in this overview to those additional components of the climate system which are most intimately coupled with the ocean, namely sea ice (which will be simply regarded as a component of the ocean circulation) and the carbon cycle, whose close interaction with the climate system has been convincingly demonstrated by the Vostok ice core data (Lorius et al., 1985; Barnola et al., 1987; Jouzel et al., 1987; Chappellaz et al., 1990).

An important sub-component of the ocean-atmosphere system is the air-sea interface. The interaction of the ocean with the climate system is controlled almost entirely by the fluxes through this surface. Fig. 1 shows the principal air-sea fluxes, the ocean variables which control these fluxes on the oceanic side of the interface, and the models which are needed to compute them. In addition to a general circulation model of the global ocean and a global ocean carbon-cycle model, a dynamical model of the air-sea interface itself, i.e., a global wave model, is also needed. It will be shown below that the ocean circulation (and thereby the coupled ocean-atmosphere system) is highly sensitive to the description of the air-sea fluxes. An improved representation of the processes at the air-sea interface using a realistic dynamical interface model is therefore an important requirement of coupled ocean-atmosphere modelling.

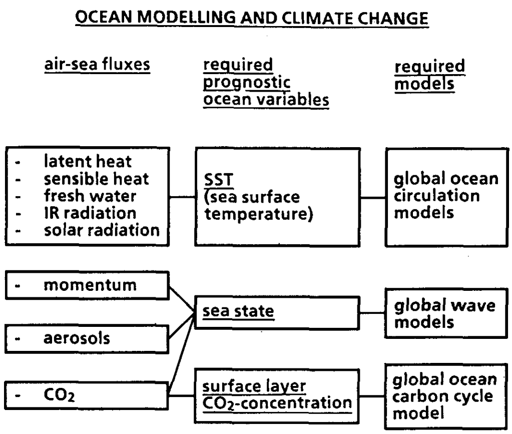

Fig. 1. Air-sea fluxes, controlling ocean air-sea flux variables and ocean models needed to compute air-sea fluxes.

The integration of global wave models in coupled ocean-atmosphere models is desirable also for the analysis, assimilation and application of global satellite data in climate models. In the present decade sea surface data from ocean satellites such as ERS-1/2, TOPEX-POSEIDON, SPINSAT, RADARSAT and ADEOS could significantly improve our understanding of the rôle of the oceans in climate, provided we develop the necessary sophisticated tools to properly exploit these powerful data sources.

To provide a reasonably self-consistent description of the dynamics of climate in the 10^{-1}–10^{3} time-scale range, an important step would therefore be the development of coupled ocean-atmosphere-surface wave-carbon cycle models. Through the rapid advances in computer technology and recent progress in the development of realistic models of all of the four sub-systems, this goal no longer appears as utopian today as it may have appeared only a few years ago. Various coupling experiments with sub-sets of these model components are already in progress. I shall attempt to review in this paper the state of modelling of the sub-systems ocean circulation, surface waves and ocean carbon cycle and describe some preliminary results of coupling experiments.

2. Simulations of the ocean response to surface forcing with the Hamburg large-scale geostrophic model

The resolution of global ocean general circulation models (O-GCMs) and atmospheric general circulation models (A-GCMs) currently used for climate studies are generally comparable. However, because of the much smaller internal Rossby deformation scale in the oceans, ocean circulation models, in contrast to atmospheric general circulation models, cannot yet resolve quasi-geostrophic (baroclinic) eddies on a global scale. Fortunately, it appears that the principal features of the world ocean circulation can nevertheless be reproduced reasonably well with non-eddy resolving models, despite the fact that in the atmosphere baroclinic eddies are essential for maintaining the mid-latitude westerlies and the basic structure of the global atmospheric circulation. Presumably, this is because the ocean circulation is much more strongly controlled by meridional boundaries, and oceanic eddies, although relatively energetic, are of much smaller scale and thus presumably have inherently small mixing-length scales. The main deficiencies of present global O-GCMS appear in the western boundary current regions, where the lack of eddy dynamics and the inadequate mean flow resolution lead to an underestimation of the maximum transports and recirculation systems. However, the main gyres of the ocean, the abyssal circulation, residence times, tracer distributions and the general structure of the global ocean "conveyer-belt" picture (Broecker and Peng, 1982; Gordon, 1986) are reproduced fairly realistically (Bacastow and Maier-Reimer, 1990; Toggweiler et al., 1989a, b).

Earlier global ocean circulation models suffered from an overestimation of the main thermocline depth (by a factor of order two) and too low salinity levels in the deep ocean (Bryan, 1969; Bryan and Lewis, 1979; Bryan, 1979; cf. also Toggweiler et al., 1989a). To circumvent these shortcomings, they were often run in the "robust-diagnostic" mode, in which the temperature and salinity fields were artificially restrained to remain close to the observed fields (Samiento and Bryan, 1982). However, it now appears likely that these deficiencies did not represent inherent shortcomings of coarse resolution models, but resulted partly from inadequacies of the particular numerical schemes or parametrizations used (for example in the treatment of horizontal and vertical mixing) and partly—as will be shown below—from a strong sensitivity of the model circulation to the precise specification of the surface forcing (K. Bryan, personal communication; Maier-Reimer and Mikolajewicz, 1989).

2.1. *Surface forcing sensitivity experiments*

The strong sensitivity of the ocean circulation to changes in surface boundary conditions has been demonstrated in a series of response experiments with the Hamburg Large Scale Geostrophic (LSG) model (Maier-Reimer, personal communication). One of the purposes of the experiments was to determine which formulation of the surface boundary conditions yielded the best simulation of the observed world ocean circulation. A particularly strong sensitivity was found with respect to the heat exchange in high latitudes. With an appropriate choice of this boundary condition, a reasonable global ocean circulation could be reproduced which was free of most of the traditional shortcomings of coarse resolution global ocean models.

The experiments were made with an 11-layer model with 3.5° × 3.5° horizontal resolution. The model uses an implicit integration scheme permitting a time-step of one month. Details of the model are given in Maier-Reimer and Hasselmann (1987) and Maier-Reimer and Mikolajewicz (1989).

Fig. 2 shows the differences of 6 characteristic

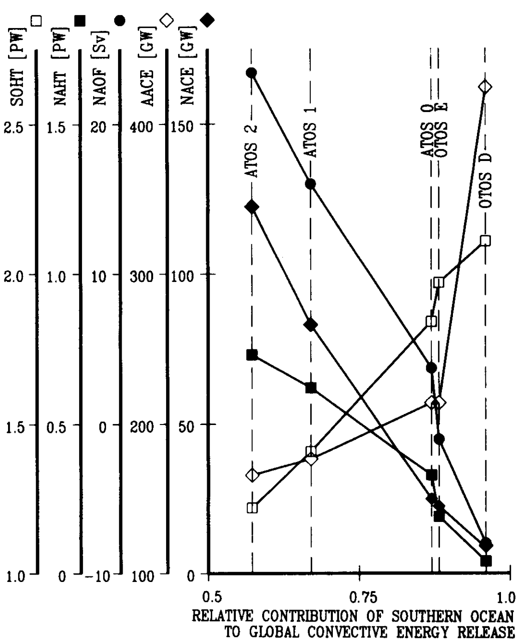

Fig. 2. Sensitivity of ocean circulation to different surface forcing (for details of forcing, see text). Experiments are stratified with respect to Southern Ocean convective energy release. Ocean circulation indices: SOHT = Southern Ocean Heat Transport; NAHT = North Atlantic Heat Transport; NAOF = North Atlantic Outflow of deep water; NACE = North Atlantic Convective Energy release, AACE = Antarctic Convective Energy release.

circulation indices computed for five different surface forcing parameterizations.

The experiments are stratified with respect to the ratio of the convective energy release in the Southern Ocean to the convective energy release in the North Atlantic, which is plotted on the x-axis. The convective energy release may be regarded as a measure of the total rate of deep water formation through convective overturning. The remaining five circulation indices, plotted against 5 different y-axis scales, represent the convective energy release in the North Atlantic (NACE) and Antarctic (AACE), the northward heat transport in the North Atlantic (NAHT), the total southward heat transport in the Southern Oceans (SOHT), and the southward deep-water outflow of the North Atlantic (NAOF).

The differences in the circulation regimes may be attributed to the different relative rates of deep-water formation in the North Atlantic and in Antarctica. The experiments represent a continuous transition from a circulation regime in which most of the deep water is formed in Antarctica and flows northward in all ocean basins (on the right side of the diagram) to a circulation regime more similar to the present "conveyer belt" circulation, in which deep water is formed mostly in the North Atlantic and flows southward out of the Atlantic into the Southern Ocean, and from there northwards slowly into the Pacific (on the left side of the figure). The closest agreement with the observed circulation was found for the experiment ATOS 1.

The transition in the circulation regime clearly has a major impact on all characteristic ocean circulation indices, including indices, such as the heat transport, which strongly affect climate. Compared with their effect on the ocean circulation, the differences in surface forcing in the five experiments shown were none the less relatively minor. Any of the five forcing parameterizations could have been justified as a reasonable estimate of observed fluxes (many have, in fact, been used in previous ocean circulation simulations).

Common factors of the boundary conditions in all experiments were the use of Hellerman and Rosenstein (1983) winds for the surface-stress forcing, the computation of the surface fresh water and heat fluxes from prescribed external salinity and temperature fields using Newtonian coupling expressions, and the use of the observed surface layer salinity, averaged over 20 m depth, as the external salinity field (Levitus, 1982). The experiments differed in the choice of the Newtonian feedback factors with which the prognostic model surface layers were coupled to the external fields and, more importantly, in the definitions of the external temperature field used to drive the heat fluxes.

Two simulations were also made without a sea ice model. These correspond to the two experiments OTOS (ocean temperature/ocean

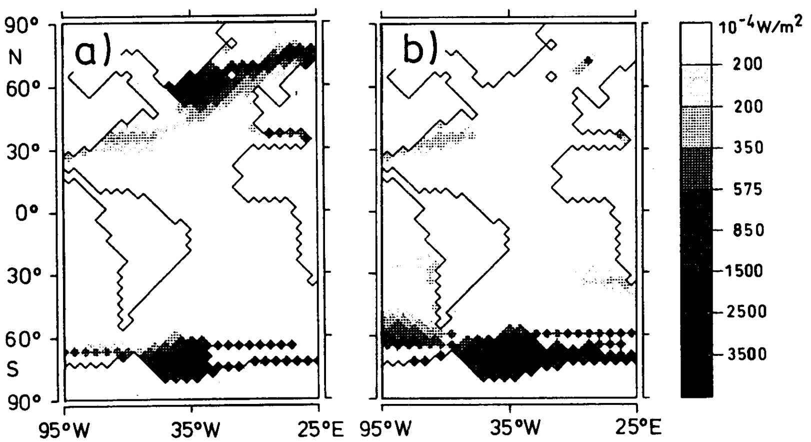

Fig. 3. Convective energy release in the Atlantic at beginning (panel a) and end (panel b) of Younger Dryas event for simulation L022 (cf. Fig. 5) (adapted from Maier-Reimer and Mikolajewicz, 1989).

salinity) D and E on the furthermost right in Fig. 2, which yielded the highest Southern Ocean convective energy release (lowest North Atlantic deep-water formation). In these cases, the observed sea-surface temperature (in the presence of sea ice: below the ice cover) was used as prescribed external temperature field.

The lowest values for the Southern Ocean convective energy release (highest North Atlantic deep water formation) were obtained in the two leftmost experiments ATOS 1 and 2 in Fig. 2, in which a modified effective surface air temperature was taken as external temperature field. This was computed by adding to the observed monthly mean air temperature an advective correction term parameterizing the heat transfer by sub-resolution scale synoptic disturbances. The advective term was set proportional to the mean air temperature gradient and the along-gradient mean wind speed component.

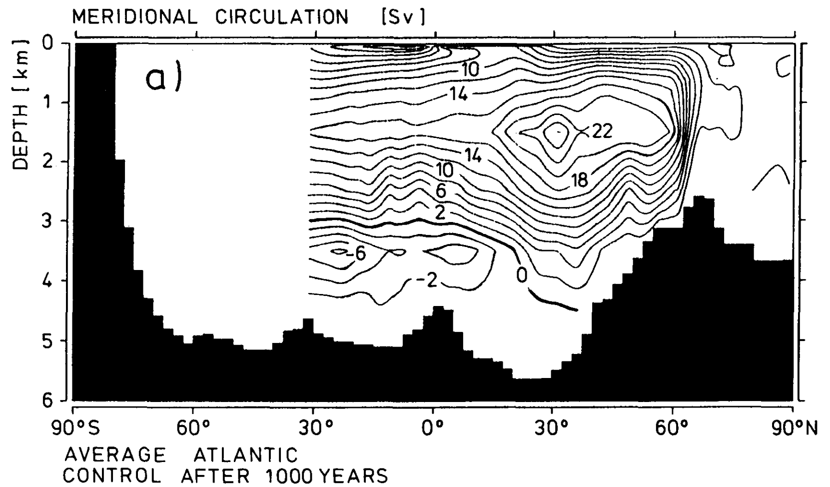

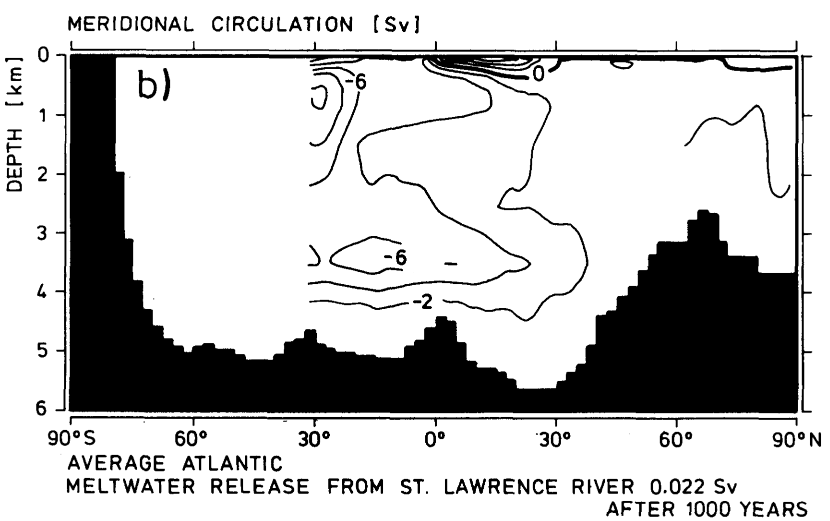

Fig. 4. Meridional Stream function of North Atlantic at beginning (panel a) and end (panel b) of Younger Dryas for experiment L022 (cf. Fig. 5) (adapted from Maier-Reimer and Mikolajewicz, 1989).

The strong sensitivity of the ocean circulation to relatively minor changes in the high latitude heat exchange, or, more generally, buoyancy flux, found in these experiments is demonstrated also in the simulations described in the following two subsections. Here similar changes in the structure of the ocean circulation are induced by modifications of the fresh water flux.

2.2. *Younger Dryas experiment*

It has been speculated by several authors (Broecker et al., 1985; Berger and Vincent, 1986; Berger and Killingley, 1982; Broecker et al., 1988) that the sudden interruption of the post-glacial holocene warming during the Younger Dryas event was caused by a change in the Atlantic ocean circulation brought about by an influx of ice sheet melt-water. A series of experiments carried out by Maier-Reimer and Mikolajewicz (1989) supports this hypothesis.

The ocean circulation was found again to be highly sensitive to the mechanism of deep water formation in high latitudes. The initial circulation in the experiments was assumed to correspond to the present day circulation, characterized by a relatively strong southward deep water transport out of the North Atlantic of about 20 Sverdrup feeding the global "conveyer belt" (Gordon, 1986; Broecker and Peng, 1982). The introduction of light fresh melt-water in the surface layer of the North Atlantic inhibited the formation of deep water. This produced a transition in the structure of the Atlantic abyssal ocean circulation to a regime more typical of the present-day Pacific circulation, in which deep water is formed primarily in Antarctica, and the deep circulation in the northern sector of the basin is almost stagnant. At the end of the Younger Dryas event, after the melt-water influx had been cut off through the build-up of new ice sheets, the ocean circulation presumably switched back to the present-day state. This phase was not included in the simulation.

Fig. 3 shows the depth of convective events in the Atlantic (which may be regarded as an alternative index of deep water formation) at the beginning and end of the Younger Dryas event. The deep-water formation in the North Atlantic is seen to be strongly reduced after the event. The corresponding change in the meridional stream function of the North Atlantic is shown in Fig. 4, illustrating the break-down of the deep circulation associated with the reduction of deep-water formation.

The reduction in the meridional mass transport

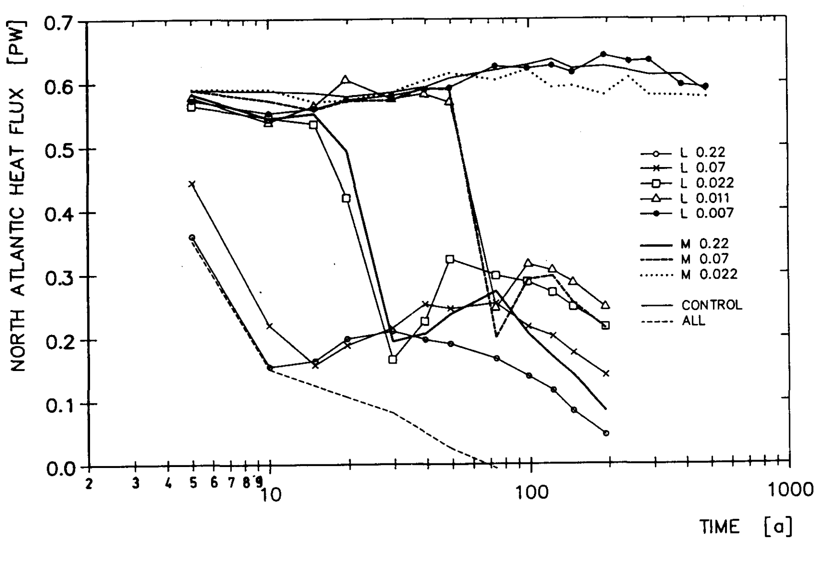

Fig. 5. Evolution of heat transport during Younger Dryas event for a series of simulations corresponding to different locations (L = St. Lawrence, M = Golf of Mexico) of fresh water influx (given in Sverdrup)(from Maier-Reimer and Mikolajewicz, 1989).

is accompanied again by a strong reduction of the northward heat transport in the Atlantic. Fig. 5 shows the evolution of the heat transport (more precisely: the total heat transfer across the air-sea interface north of 30° N in the Atlantic) for a series of simulation experiments corresponding to different rates and geographical locations of the fresh-water influx (L denotes St. Lawrence outflow, M. Missippi outflow; numbers denote influx in Sverdrup). The transition in the circulation regime is seen to occur on a relatively short time scale of a few decades. Curve L 022, for example, showing a rapid transition after about 30 years, is based on reasonably realistic estimates of the melt-

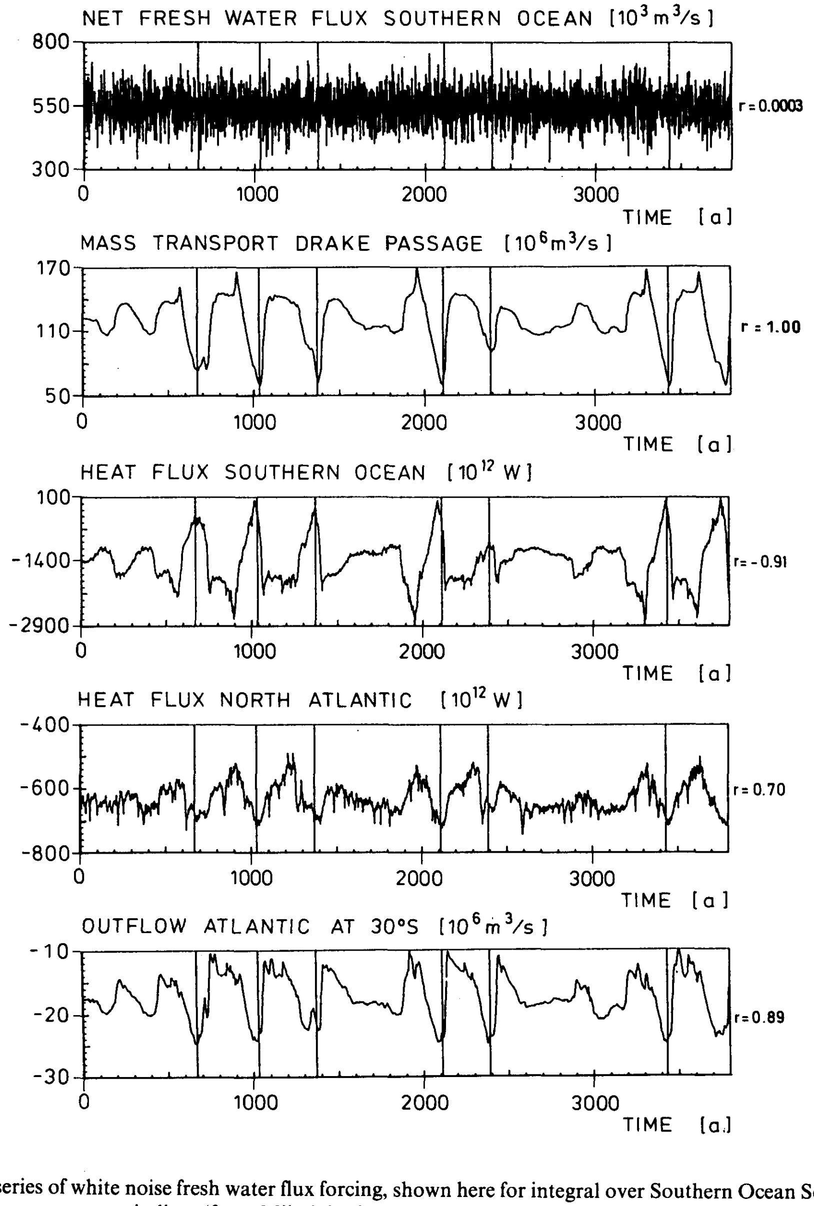

Fig. 6. Time series of white noise fresh water flux forcing, shown here for integral over Southern Ocean South of 30° S, and various ocean response indices (from Mikolajewicz and Maier-Reimer, 1990).

water influx rate of 0.022 Sverdrup (corresponding to a decrease of the Laurentide ice sheet of approximately 0.35 m/year). A reduction of the melt water influx by a factor of two (L 011) merely delays the transition by the same factor. (The transition of the deep ocean circulation is less rapid than the heat flux change.)

In addition to changes in the net influx of fresh water through the continental run-off of ice sheet melt water, a change in the ocean circulation regime could, of course, also have been triggered by changes in the distribution of the surface fresh water flux (precipitation minus evaporation) or in the surface wind. The latter could modify the horizontal advection of low salinity surface waters into the regions of deep water formation (Stigebrandt, 1985). It would be of interest to explore these alternative hypotheses through further O-GCM experiments.

The impact of the computed reductions in the North Atlantic heat transport during the Younger Dryas event on the northern hemispheric climate, particularly in Europe, must have been dramatic. The further evolution of the Younger Dryas event after the transition to a new circulation regime can be pursued only with coupled ocean-atmosphere model simulations, but the ocean model experiments themselves already clearly demonstrate the important rôle of the ocean in controlling climate sensitivity.

2.3. *Response of the ocean circulation to stochastic forcing*

A 3rd example, finally, demonstrating the sensitivity of the ocean circulation to surface forcing is an experiment by Mikolajewicz and Maier-Reimer (1990) on the response of the global ocean circulation to white noise stochastic forcing. It has been pointed out by Mitchell (1966) and Hasselmann (1976) that many of the qualitative features of long-term climate variability can be explained as the response of the slow components of the climate system to the short time scale forcing by atmospheric weather variability. For the low frequencies relevant for climate variability, the atmospheric forcing can be regarded as effectively white noise. In their experiments, Mikolajewicz and Maier-Reimer limited the stochastic atmospheric forcing to the surface fresh-water flux (evaporation minus precipitation). The variability was represented as an uncorrelated white noise process in time (at the model time step resolution of one month), while a spatial correlation scale of 2500 km was assumed as the estimated scale of monthly mean weather anomaly patterns. The

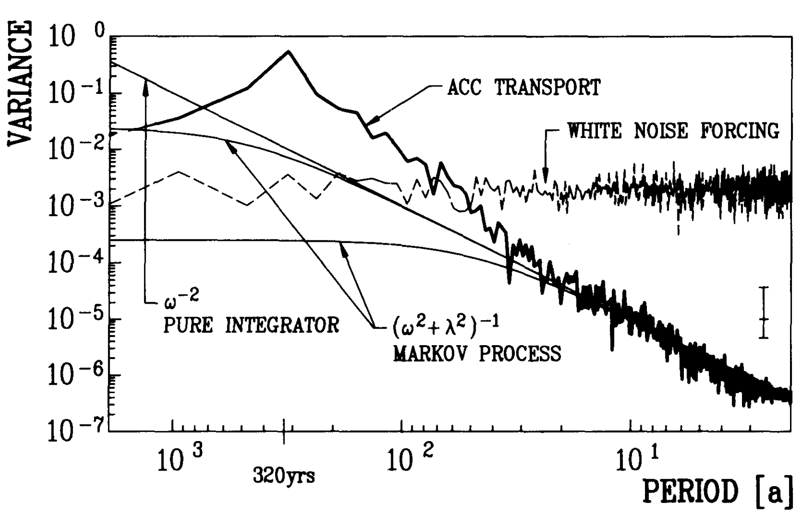

Fig. 7. Variance spectrum of time series of white noise forcing and mass transport through Drake passage shown in Fig. 6 (adapted from Mikolajewicz and Maier-Reimer, 1990).

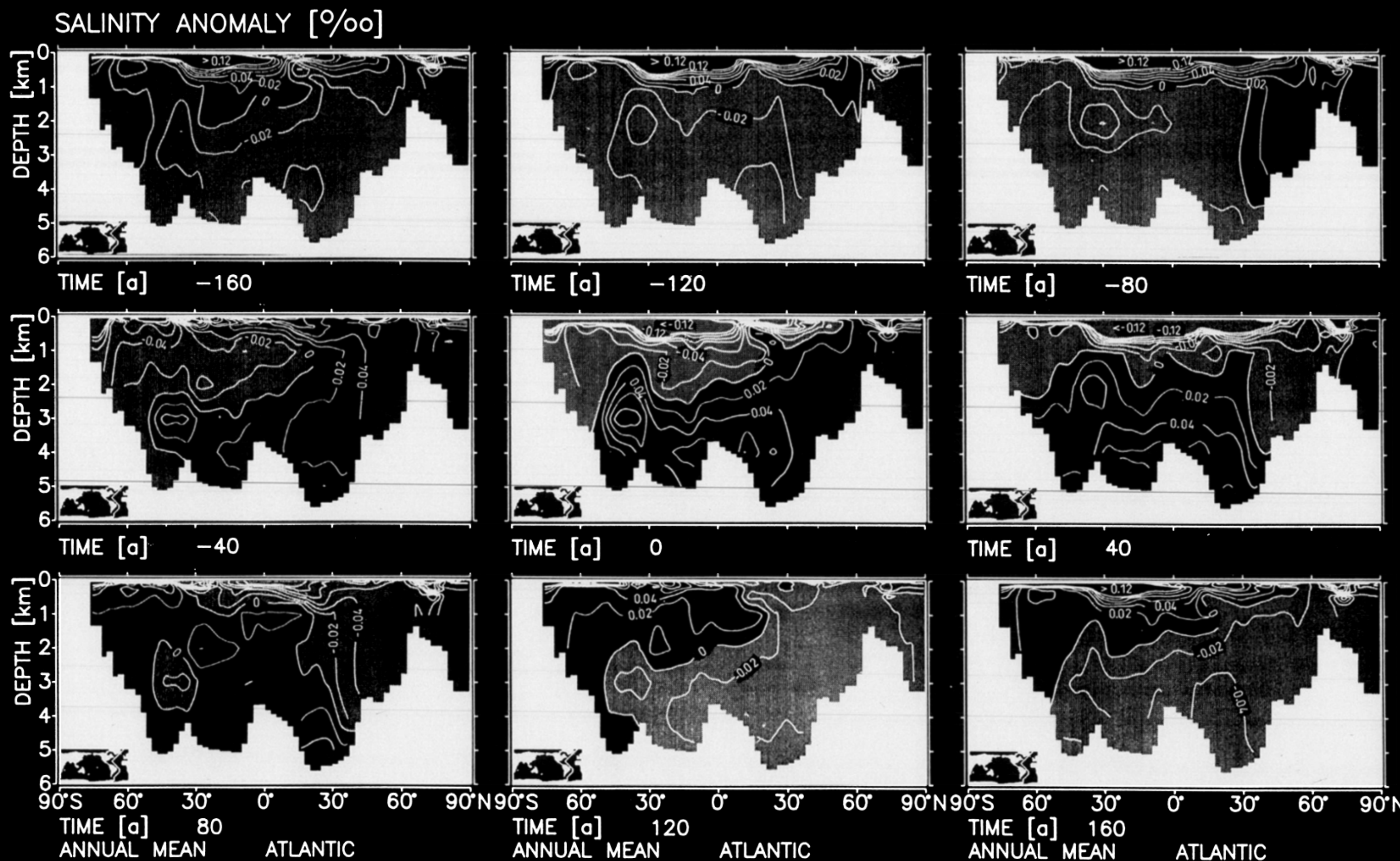

Fig. 8. Meridional section through Atlantic of salinity signal of 320-year oscillation seen in Figs. 6 and 7. The different phases of the oscillation (from −160 to +160 years) were constructed by composite analysis (adapted from Mikolajewicz and Maier-Reimer, 1990).

standard deviation of the monthly averaged fresh-water fluxes about the climatological mean was taken as 16 mm/month, corresponding to 20% of the climatological global mean precipitation (determined from Baumgartner and Reichel, 1975).

Fig. 6 shows the time series of the white-noise forcing and some characteristic indices of the oceanic response. The corresponding variance spectra of the forcing and the Antarctic Circumpolar Current transport are shown in Fig. 7. The response spectrum exhibits a peak near 320 years period, which is markedly higher than the variance spectrum of a pure integrator (ω^{-2}) or a first-order Markov process ($(\omega^2 + \lambda^2)^{-1}$, where λ is the process damping factor). The peak can be attributed to a series of discrete events seen to recur in Fig. 6 at irregular intervals of 200–400 years.

The structure of the events was determined by a composite event analysis (a more complete picture has since been constructed using a Principal Oscillation Pattern analysis, Mikolajewicz, 1990). The oscillation, shown in a vertical Atlantic section in Fig. 8, represents a rotating anomaly pattern, which is advected with the mean circulation. The 320 year period of the oscillation is consistent with estimates of the mean advective overturning time scale of the meridional Atlantic circulation.

The changes in the ocean circulation and the oceanic heat fluxes (cf. Fig. 6) generated by realistic white-noise fresh water flux variations in these experiments are significant and can again be expected to have a strong impact on climate.

3. Preliminary results with coupled ocean-atmosphere model simulations of global warming

It is generally recognized that existing simulations of the climatic response to increased greenhouse gas concentrations using atmospheric general circulation and mixed layer ocean models can yield only estimates of the expected global warming. The inadequate simulation of the deep ocean below the mixed layer in such experiments implies that both the transient response, which is strongly affected by the oceanic heat uptake, and the final equilibrium state, which is modified by the changes in the mean oceanic heat transport, cannot be correctly simulated.

Although global O-GCMs have been available almost as long as A-GCMs, a number of problems have hindered the application of realistic coupled ocean-atmosphere GCMs in global warming simulations. It appears that these difficulties have now been largely overcome, however, and several modelling groups are beginning to seriously pursue coupled model studies. The main hindrances to the application of coupled O-A-GCMs in the past have been the following.

(1) Questions regarding the reliability of ocean circulation models (too deep main thermocline and errors in deep ocean properties). These has now been largely resolved through improvements in the numerics, in the representation of diffusion and in the surface forcing boundary condition.

(2) The tendency for coupled models to drift into a climate state which differs too strongly from the present climate to be used as a reference state. This technical difficulty has been largely resolved through the introduction of the flux-correction method (Sausen et al., 1988). (Although balanced in the flux correction method, the residual model errors, which are the basic cause of model drift, nevertheless merit attention).

(3) The high computer costs of running coupled O-A-GCM simulations at acceptable resolution over long periods of many decades or centuries. This problem has been alleviated through advances in super-computers. However, computing expense is still a major limitation and has so far prohibited coupled O-A-GCM simulations from being extended into the multi-century-millenium time scale range needed to investigate the evolution of the coupled ocean-atmosphere system beyond the initial response stage.

Similar global warming simulations with coupled ocean atmosphere models have now been made by three different research groups: the National Center of Atmospheric Research (Washington and Meehl, 1989), the Geophysical Fluid Dynamics Laboratory (Stouffer et al., 1989) and the University-Max Planck group in Hamburg. The Hamburg Group carried out two coupled ocean-atmosphere experiments using the Hamburg climate version (ECHAM) of the European Centre for Medium Range Weather

Forecasts atmospheric model (Roeckner et al., 1989) and two different ocean models: the LSG model referred to in the previous section, and an isopycnal model (Oberhuber, 1990). (Data from these experiments has been kindly made available by the Hamburg group prior to the publication of their results, presently in preparation.) One of the scenarios considered by all groups was an extrapolation of the present rate of increase of the equivalent CO_2 concentration (defined as the CO_2 concentration with the same net radiative forcing at the surface as all anthropogenic greenhouse gases combined). Washington and Meehl assumed a 1% linear increase, Stouffer et al., a 1% exponential increase and the Hamburg group the "business-as-usual" scenario A of the Intergovernmental Panel on Climate Change (Houghton et al., 1990), which corresponds to an approximately 1.3% exponential increase. The Hamburg group also carried out a simulation for an IPCC reduced emission scenario D.

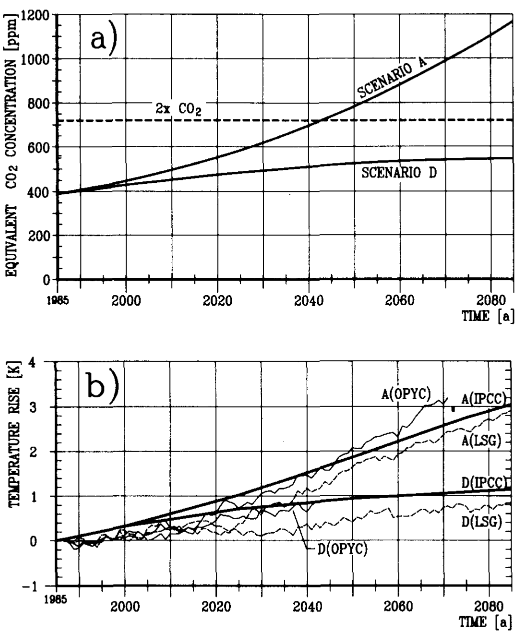

Fig. 9. Evolution of equivalent CO_2 concentration according to IPCC business-as-usual scenario A and reduced emission scenario D (panel a) and resulting global mean temperature computed with the Hamburg coupled ocean-atmosphere model (LSG) and estimated by IPPC Working Group 1 using a box diffusion upwelling model (IPPC) (panel b).

Fig. 9 shows the growth in equivalent CO_2 according to the IPCC scenarios A and D (panel a) and the corresponding increases in global mean temperature computed by the Hamburg O-A-GCM simulations, using the LSG ocean model, for the first 100 years of the integration (panel b). Also shown are the IPCC Working Group 1 predictions using a simple box-diffusion-upwelling ocean-atmosphere model. The somewhat slower initial growth of the coupled O-A-simulations compared with the box-diffusion model is probably a real effect and not due to spin-up (the experiment was switched on in 1985). In all model experiments, the strongest delay in the warming due to the heat uptake of the oceans occurs in the southern hemisphere. This is because the oceans cover a much larger fraction of the earth's surface in the southern hemisphere and heat can be efficiently transported into the deep ocean in a large region along the Antarctic Circumpolar Current through deep convective mixing. The North-South asymmetry is evident in the Hovmöller diagram (Fig. 10) showing the evolution of the zonally-averaged temperature for the Hamburg scenario A simulation (see also Stouffer et al., 1989, Fig. 2).

The models were not integrated long enough to distinguish clearly between the delay effects due to the heat uptake of the oceans and the modifications in the asymptotic equilibrium state due to changes in the mean ocean heat transport. However, regions of cooling seen in the global temperature distribution (not shown), for example in the Southern Ocean, are most likely due to changes in the circulation pattern rather than the heat uptake.

Since the ocean can only delay the global warming and redistribute the heat within the system, it is often assumed that to first order the ocean has no effect on the global mean equilibrium temperature increase. However, this is true only if no unstable transition to another equilibrium climate state occurs. The Younger Dryas experiment and a number of recent investigations on multi-equilibrium ocean circulation states (Bryan, 1986; Welander, 1986; Marotzke et al., 1988; Manabe and Stouffer, 1988) indicate that this possibility cannot be ruled out. The question can be resolved only through more extended integrations with realistic coupled O-A-GCMs.

As pointed out above, available computer

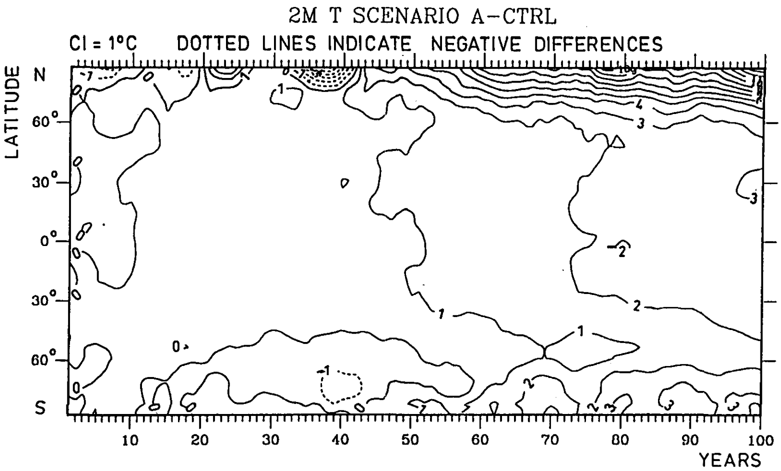

Fig. 10. Evolution of zonally averaged surface (2 m height) air temperature computed with the Hamburg ECHAM-LSG coupled atmosphere-ocean model for scenario A.

capacity is unfortunately still a limiting factor in such simulations. Various proposals have been made for extending the range of integration by using burst integration techniques (Hasselmann, 1988) or other acceleration methods (e.g., Bryan, 1984). However, these are still in the exploratory stage for coupled ocean-atmosphere models and further research will be needed to extend such simulations to the full dynamic time scale range of the ocean.

4. Models of the air-sea interface

In present coupled ocean-atmosphere models, the complex air-sea interaction processes at the ocean-atmosphere interface are normally parameterized in terms of simple bulk formulae. The dynamics of the surface wave interface, and the interactions of surface waves with the oceanic and atmospheric boundary layers on either side of the interface, are not considered. The demonstrated sensitivity of the ocean circulation to the details of the surface forcing, however, implies that a more careful treatment of the air-sea fluxes is called for.

Encouraging progress in surface wave modelling in recent years has now provided a firmer physical basis for a reassessment of air-sea coupling mechanisms. In the third generation wave model developed by the WAM (WAve Modelling) group, the evolution of the surface wave spectrum has been computed for the first time from the basic physical source functions which govern the spectral energy balance, without additional ad hoc assumptions regarding the shape of the spectrum (WAMDIG, 1988). The source functions describe not only the energy and momentum balance of the wave field, but also the transfer of momentum and mixing energy from the atmosphere to the upper layer of the ocean. Atmospheric boundary layer models which explicitly compute the interaction of the surface wave field with the atmospheric boundary layer, including the fluxes of sensible and latent heat as well as the momentum and kinetic energy fluxes, are currently being developed (Janssen et al., 1989; Janssen, personal communication).

The impact of surface wave dynamics on the air-sea fluxes is illustrated in Fig. 11, which shows the global distribution, at a given synoptic time, of the ratio of the wave induced momentum transfer, computed with the WAM model, to the total momentum transfer into the ocean, computed using the standard Charnock drag law. In regions of intense storms (in the present case in the Southern Ocean), a significant fraction (30–50%) of the estimated total momentum transfer goes into the surface wave field. In bulk aerodynamic drag laws, this component is either neglected or simply absorbed in the net drag coefficient. However, the wave-induced momentum transfer cannot be

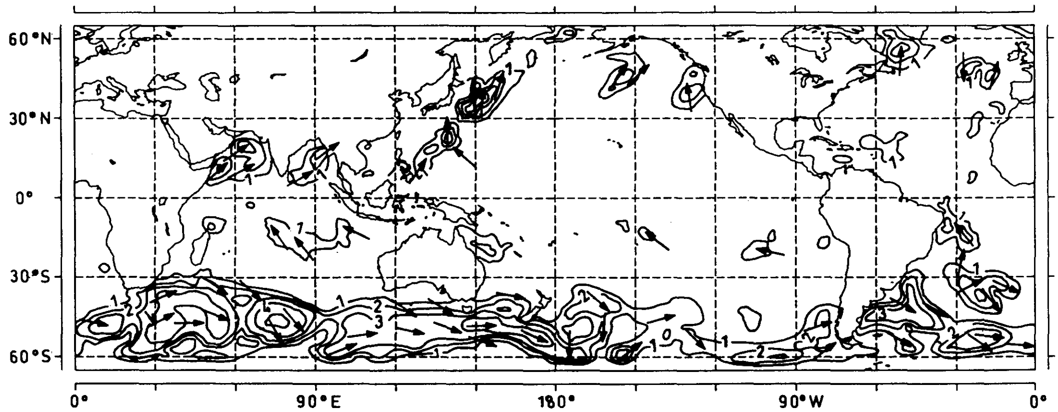

Fig. 11. Ratio of wave induced stress computed with WAM model to total stress computed according to the Charnock formula. Isoline units are in tenths.

captured in a local drag law dependent only on the local wind speed. It also depends on the local wave spectrum, which is a function of the entire past space-time history of the wind field. An improved representation of the momentum transfer is therefore possible only through the application of a wave model.

In addition to the need for a better physical representation of ocean-atmosphere coupling, surface wave models are needed also to properly interpret and analyse ocean satellite data. We look forward in the nineties to continuous global measurements of important sea surface properties from microwave sensor systems aboard a variety of ocean satellites: measurements of the sea surface topography, significant wave height and surface wind speed with altimeters; estimates of the surface wave spectra from synthetic aperture radar images; and measurements of the surface wind velocity from scatterometers. Most of these microwave sensor signals, however, can be properly interpreted only with the aid of models describing the detailed interactions between the atmospheric boundary layer, the ocean wave spectrum and the short backscattering ripple waves. The sophisticated inversion algorithms needed to derive surface wind and ocean wave properties from these models require as input first-guess information. This can be provided only by atmospheric general circulation models and global wave models.

These considerations imply the need for a comprehensive data assimilation system of the general structure indicated in Fig. 12 (Hasselmann, 1985). The close interaction between the different stages of the analysis: provision of first-guess data; application of sensor algorithms; assimilation of

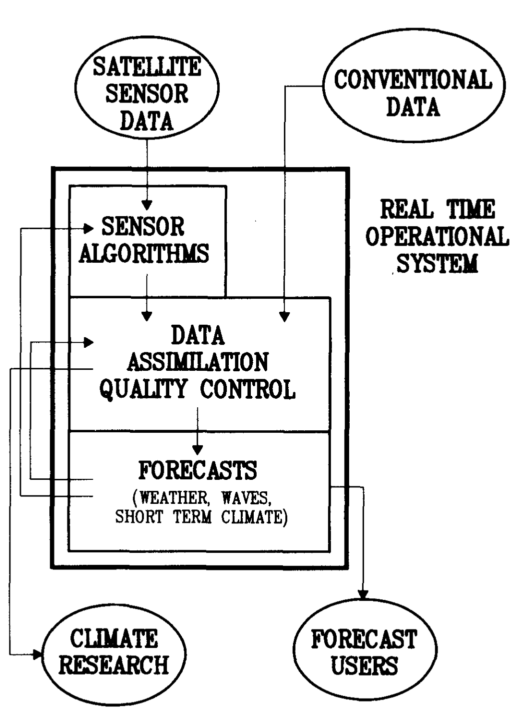

Fig. 12. Structure of comprehensive data assimilation system for processing satellite wind and wave data together with conventional weather station data.

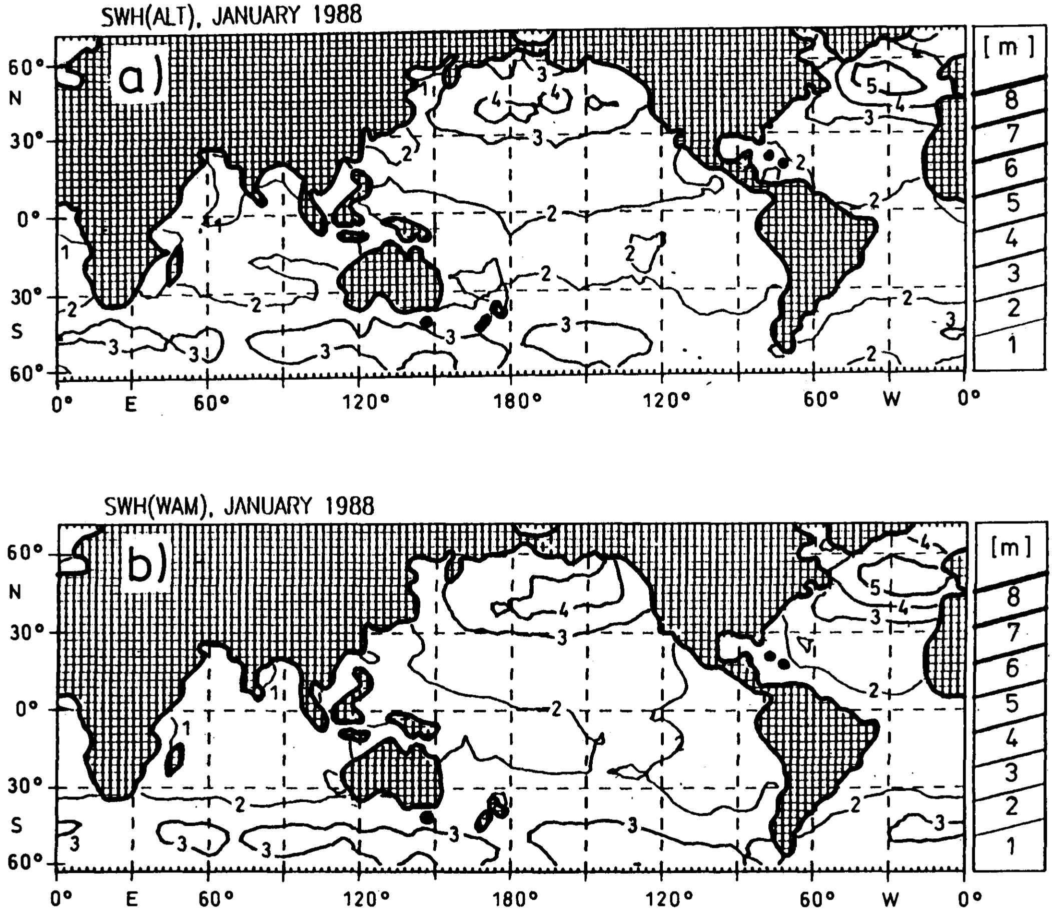

Fig. 13. Comparison of mean significant wave heights for January 1988 derived from the GEOSAT altimeter (panel a) and the WAM wave model (panel b) (from Romeiser, 1991).

the satellite data together with conventional observing system data in the models; and the actual forecast, demands that all analysis levels should be incorporated within a single system. To keep up with the continuous data inflow, the entire operation must furthermore be run in quasi-real time. This requires implementation in an operational forecasting installation.

Fig. 13 gives an indication of the quality of wave data which satellites can provide today and the skill of modern wave model computations. Panel (a) shows the mean significant wave height for January 1988 derived from the GEOSAT altimeter, while panel (b) shows the significant wave height predicted by the WAM 3rd generation wave model for the same period, using the analysed wind fields of the European Centre for Medium Range Weather Forecasts (Romeiser, 1991).

The agreement of the monthly mean fields is remarkable. However, an inspection of individual synoptic weather situations normally reveals regional discrepancies. These can generally be attributed to inaccuracies in the analysed wind field. The implementation of a combined wind and wave data assimilation scheme would enable these wind-field errors to be corrected, thereby improving not only the weather and wave forecasts, but also the analysed air-sea flux fields provided for climate studies.

5. Simulations with the Hamburg ocean carbon cycle model

The ocean plays an important rôle in the climate system not only through the storage and transport of heat, but also through the storage and transport of CO_2. The ocean contains approximately 60 times as much CO_2 as the atmosphere (and the living terrestrial biosphere). Although reduced through the bicarbonate buffering factor, the storage capacity of the oceans for incremental changes in CO_2 is still approximately 7 times greater than that of the atmosphere.

The fact that the estimated air-borne fraction of past industrial emissions of CO_2 is approximately 50%, rather than 15% as predicted for an equilibrium incremental change, must be attributed to the large CO_2 response time of the oceans. This is largely governed by the rate of transfer of CO_2 from the surface layer of the ocean into deeper layers. This in term depends critically on the structure of the deep ocean circulation, which, as has been pointed out, is highly sensitive to changes in the surface forcing. It follows that a reliable prediction of future CO_2 concentrations in the atmosphere for a given time-dependent CO_2 emission scenario, together with the computation of the resulting climate change, requires a comprehensive coupled model including all three major interacting components: the atmospheric and oceanic circulation, and a realistic three dimensional model of the ocean carbon cycle based on a dynamic ocean model.

The strong interaction between climate and the carbon cycle has been underscored through the recent discovery in ice core data of significant changes in past atmospheric CO_2 concentrations. The changes were found to be highly correlated with variations in paleoclimatic temperature and other paleoclimatic indices (Barnola, et al., 1987; Jouzel et al., 1987). A number of hypotheses have been proposed to explain these variations. In view of the dominance of the ocean carbon reservoir in the global carbon cycle, most theories attribute the changes in atmospheric CO_2 content to changes in the ocean circulation or in other components of the ocean carbon system.

Heinze (1990) and Heinze et al. (1991) have

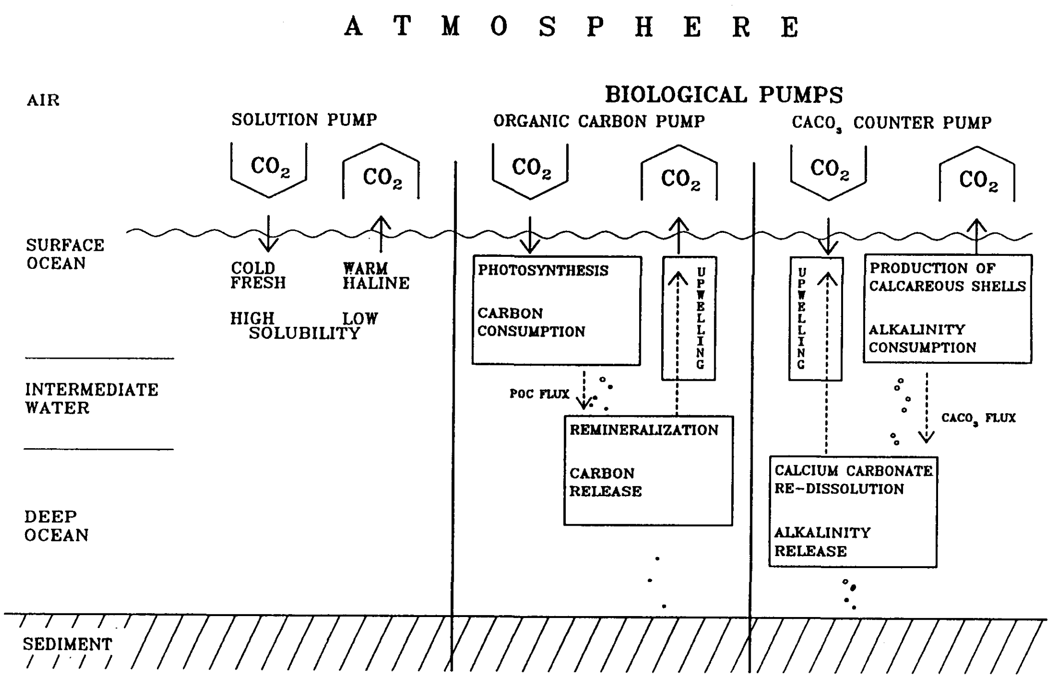

Fig. 14. Structure of the Hamburg carbon cycle model (from Heinze et al., 1991).

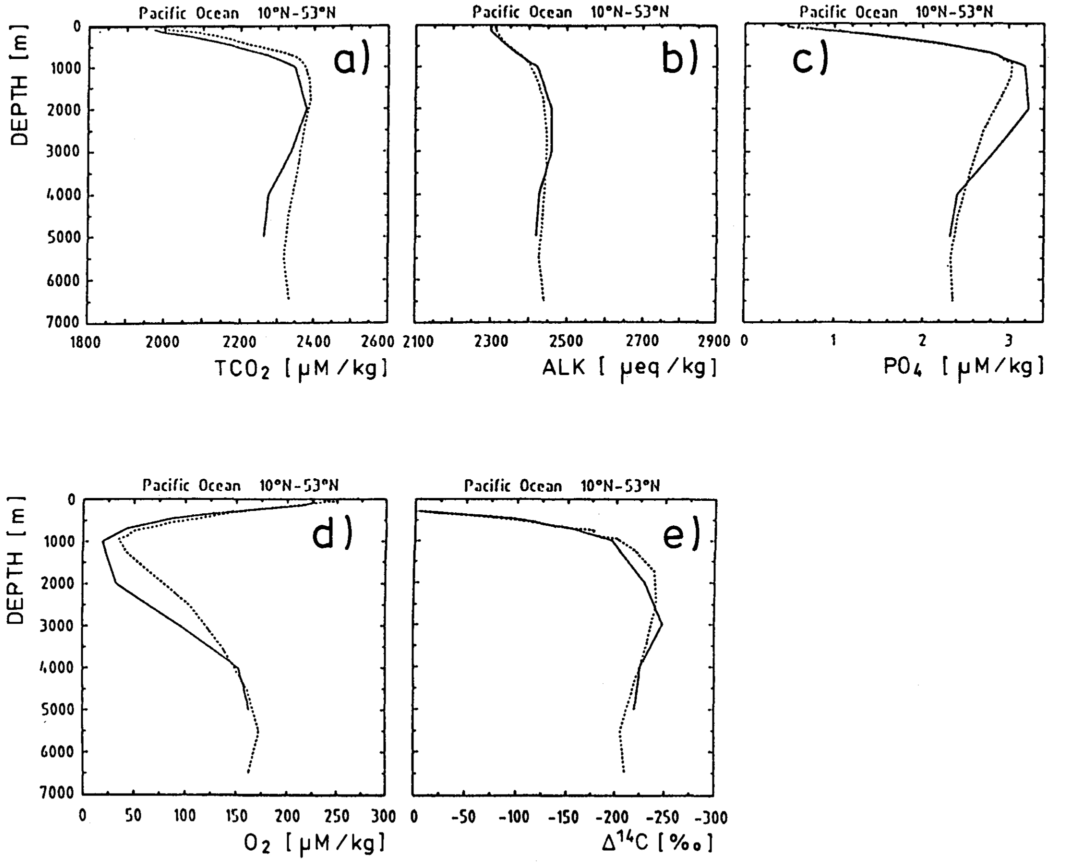

Fig. 15. Modelled (solid line) and measured (dotted line) (GEOSECS) profiles of carbon cycle constituents in the Pacific (panels a–e) and Atlantic (panels f–j) (from Bacastow and Maier-Reimer, 1990).

applied a three-dimensional carbon cycle model based on a realistic three-dimensional ocean transport model (Maier-Reimer and Hasselmann, 1987; Bacastow and Maier-Reimer, 1990) to carry out a systematic inverse modelling study of these hypotheses for the last 120,000 years. The basic elements of the carbon cycle model are shown in Fig. 14. A more detailed description is given in Bacastow and Maier-Reimer (1990). The model reproduces the observed distributions of the important constituents of the oceanic carbon cycle reasonably well (Fig. 15).

The principal results of the investigations of Heinze et al. (1991) are summarized in Figs. 16–18. Fig. 16 shows a comparison of the time series for a number of observed paleoclimatic indices and the optimal model reconstructions of these indices. The reconstructions were obtained by optimally tuning a number of externally specified model parameters during the course of the model integration. The parameters were defined such that each could be identified with a particular hypothesis regarding the cause of the variations in atmospheric CO_2 content (see Heinze, 1990; Heinze et al., 1991, for a more detailed definition of the paleoclimatic indices and model parameters). It was not possible to obtain an acceptable agreement with all observations through changes in any one single parameter alone. However, a suitable time dependent combination of parameter changes, shown in Fig. 17, reproduces the observed time series in Fig. 16 reasonably well

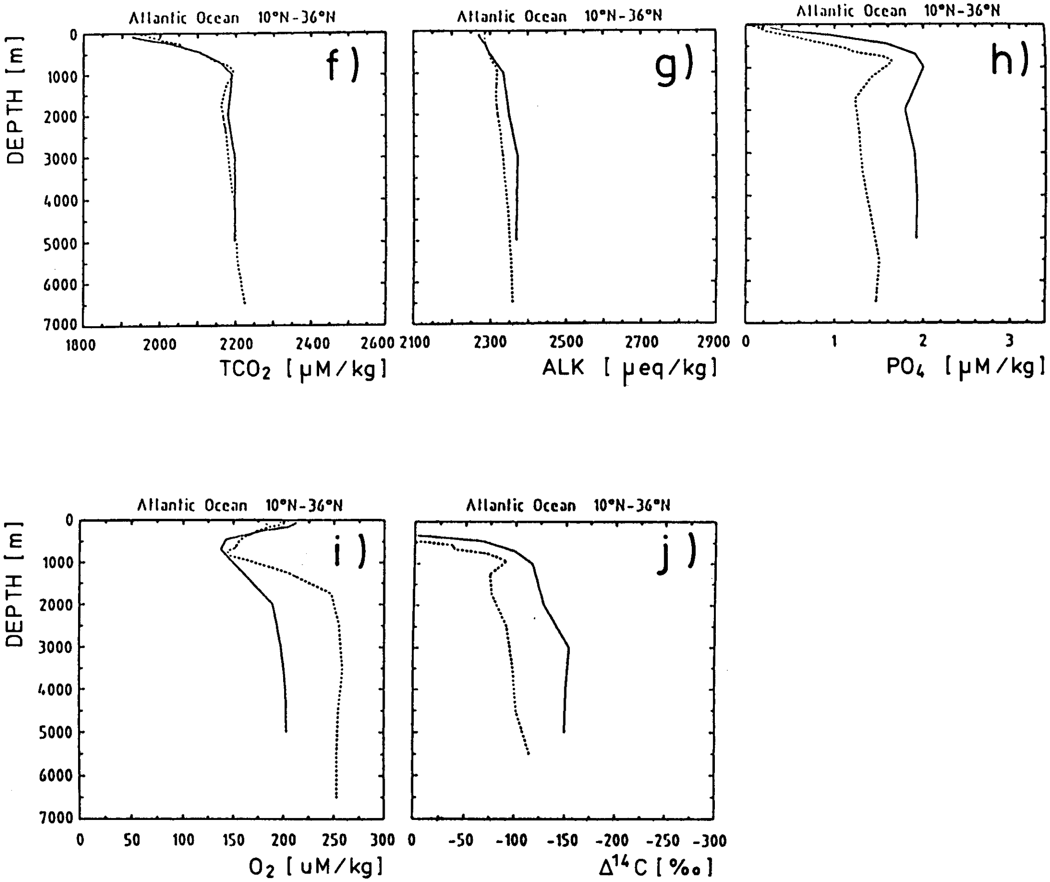

Fig. 15. Continued.

(for the particular optimal tuning run shown, some of the parameters, such as the carbon/phosphate Redfield ratio and the rain ratio, were frozen).

The separate contributions to the change in atmospheric CO_2 concentration due to individual parameter changes is shown in Fig. 18. The most important single tunable parameter is seen to be the strength of deep-ocean ventilation. However, additional parameter changes must be invoked to explain the fluctuations observed in other climatic indices.

The study demonstrates the usefulness of three dimensional carbon cyle models for unravelling complex interactions within the ocean circulation-carbon cycle system. The results illustrate also the strong interconnection between the atmospheric-oceanic circulation system and the carbon cycle and emphasize again the pivotal rôle of high-latitude convective processes in the ocean for climate.

6. Summary

The selected examples of recent simulation studies using global ocean circulation models, atmospheric models, wave models and ocean carbon cycle models demonstrate the close inter-linkage between the ocean circulation and the other principal climate sub-systems with which the ocean interacts: the atmosphere, the air-sea interface and the carbon cycle. The ocean circulation

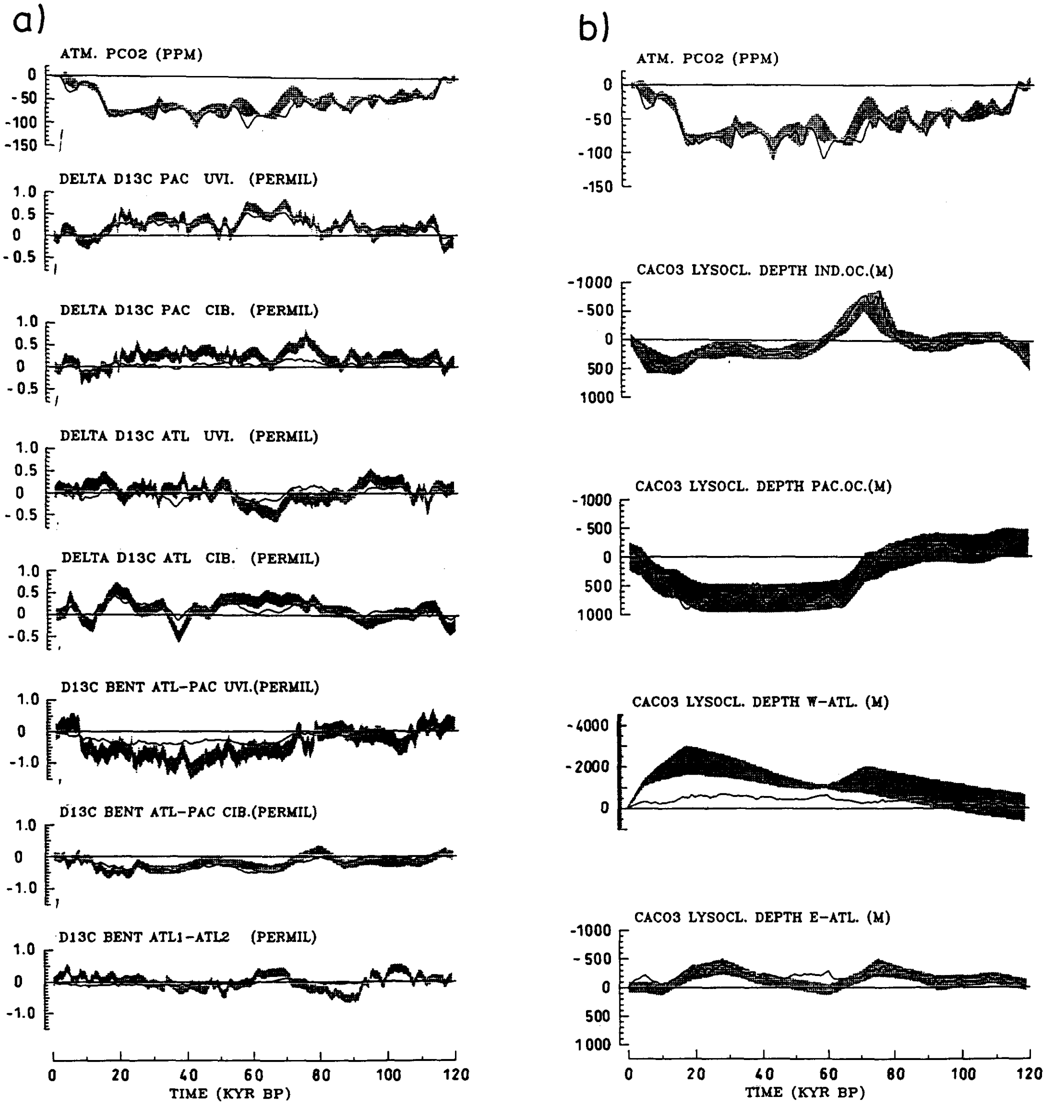

Fig. 16. Simulated and measured paleoclimatic indices for last 120 kyears for various $\Delta\ ^{13}C$ time series (panel a) and lysocline depths (panel b) in different ocean basins. Shading indicates estimated uncertainties of measurements. The simulated time series were constructed by optimal time-dependent tuning of a number of model parameters (cf. Fig. 17) representing various hypotheses which have been proposed to explain observed past CO_2 variations (from Heinze, 1990).

represents a very sensitive component within this coupled system. The dynamics of the complete system can be studied ultimately only with a fully interactive ocean-atmosphere-surface-wave-carbon cycle model. Suites of realistic sub-system models which can be used for such integrated models now exist in several laboratories. In the light of these advances and rapid developments in super-computer technology, the study of the dynamics of the climate system with more sophisticated integrated models has now become within reach.

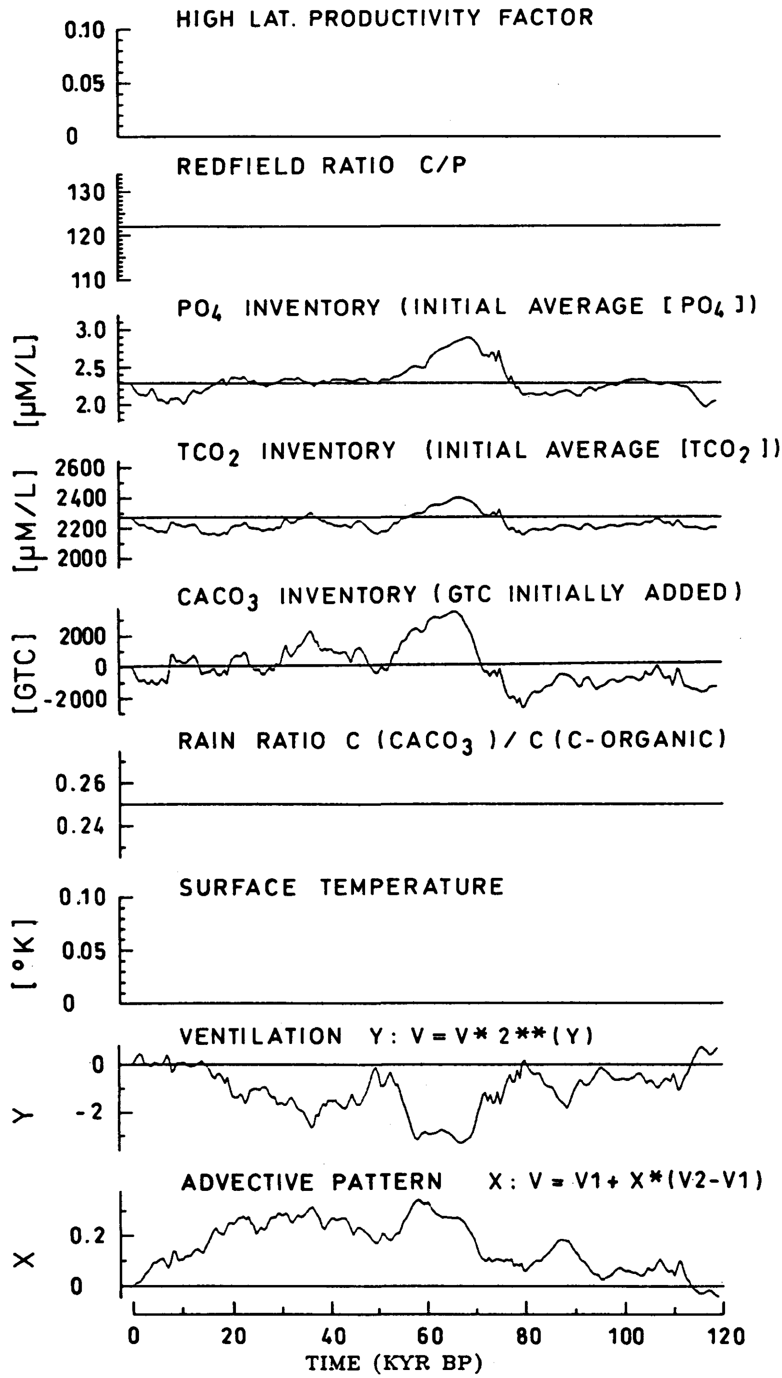

Fig. 17. Parameter changes tuned to optimally reproduce the observed paleoclimatic indices shown in Fig. 16. (Not all of the parameters were varied in this particular model simulation as indicated by the zero change curves in the first two and last but one panel) (from Heinze, 1990).

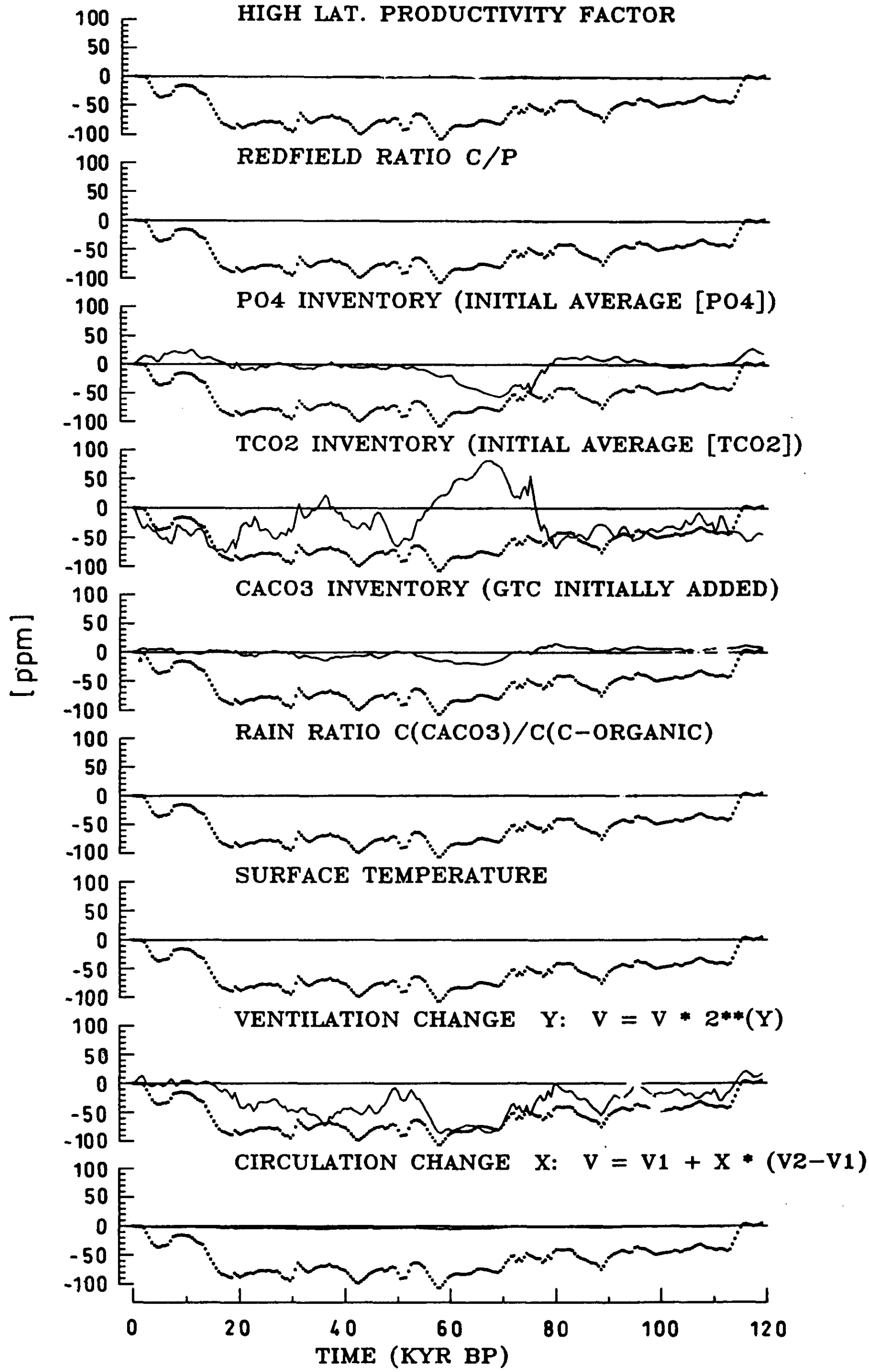

Fig. 18. Fraction of observed CO_2 changes (dotted curves) which can be explained by individual parameter changes (full lines) (from Heinze, 1990).

REFERENCES

Bacastow, R. B. and Maier-Reimer, E. 1990. Circulation model of the oceanic carbon cycle. *Climate Dynamics 4*, 95–125.

Barnola, J. M., Raynaud, D., Korotkevich, Y. S. and Lorius, C. 1987. Vostok ice core provides 160,000-year record of atmospheric CO_2. *Nature 329*, 408–414.

Baumgartner, A. and Reichel, E. 1975. *The world water balance: mean annual global, continental and maritime precipitation, evaporation and run-off.* Elsevier, 179 pp.

Berger, W. H. and Killingley, J. S. 1982. The Worthington effect and the origin of the Younger Dryas. *J. Mar. Res. 40*, 27–38.

Berger, W. H. and Vincent, E. 1986. Sporadic shutdown of North Atlantic deep water production during the Glacial-Holocene transition. *Nature 324*, 53–55.

Broecker, W. S. and Peng, T.-H. 1982. *Tracers in the Sea*, Lamont-Doherty Geological Observatory, 690 pp.

Broecker, W. S., Peteet, D. M. and Rind, D. 1985. Does the ocean-atmosphere system have more than one stable mode of operation? *Nature 315*, 21–25.

Broecker, W. S., Andree, M., Wolfi, W., Oeschger, H., Bonani, G., Kennet, J. and Peteet, D. 1988. The chronology of the last deglaciation: Implications to the cause of the Younger Dryas event. *Paleoceanogr. 3*, 1–19.

Bryan, K. 1969. A numerical method for the study of the circulation of the world ocean. *J. Comput. Phys. 4(3)*, 347–376.

Bryan, K. 1979. Models of the world ocean. *Dyn. Atmos. Oceans 3*, 327–338.

Bryan, K. and Lewis, L. J. 1979. A water mass model of the world ocean circulation. *J. Geophys. Res. 84*, 2503–2517.

Bryan, K. 1984. Accelerating the convergence to equilibrium of ocean climate models. *J. Phys. Oceanogr. 14*, 663–673.

Bryan, F. 1986. High latitude salinity effects and interhemispheric thermohaline circulations. *Nature 305*, 301–304.

Chappellaz, J., Barnola, J. M., Raynaud, D., Korotkevich, Y. S. and Lorius, C. 1990. Ice-core record of atmospheric methane over the past 160,000 years. *Nature 345*, 127–131.

Gordon, A. L. 1986. Interocean exchange of Thermocline Water. *J. Geoph. Res. 91, C4*, 5037–5046.

Hasselmann, K. 1976. Stochastic climate models, Part 1: Theory. *Tellus 28*, 473–485.

Hasselmann, K. 1985. Assimilation of microwave data in atmospheric and wave models. *Proceedings of a Conference on the Use of Satellite Data in Climate Models.*, ESA SP-244.

Hasselmann, K. 1988. Some problems in the numerical simulation of climate variability using high-resolution coupled models. *Proceedings of the North Atlantic Treaty Organization (NATO) Advanced Study Institute (ASI) on physically-based modelling and simulation of climate and climatic Change*, Part I, 11–23 May 1986, Erice, Italy. Series C: Mathematical and Physical Sciences, 243, (ed. M. E. Schlesinger), Kluwer Academic Publishers, 583–614.

Heinze, C. 1990. *Zur Erniedrigung des atmosphärischen Kohlen-dioxidgehaltes durch den Weltozean während der letzten Eiszeit.* Ph.D. Thesis, Univ. Hamburg, 180 pp. (in German)

Heinze, C., Maier-Reimer, E. and Winn, K. 1991. Glacial pCO_2 reduction by the world ocean-experiments with the Hamburg carbon cycle model. Paleoceanography 00, 000–000.

Hellerman, S. and Rosenstein, M. 1983. Normal monthly wind stress over the world ocean with error estimates. *J. Phys. Oceanogr. 13*, 1093–1104.

Houghton, J., Jenkins, G. J. and Ephraums, J. J. (eds) 1990. *Climate change.* The IPCC Scientific Assessment, Cambridge Univ. Press, 365 pp.

Janssen, P. A. E. M., Lionello, P. and Zambresky, L. 1989. On the interaction of wind and waves. *Phil. Trans. Roy. Soc. London A329*, 289–301.

Jouzel, J., Lorius, C., Petit, J. R., Genthon, C., Barkov, N. I., Kotlyakov, V. M. and Petrov, V. M. 1987. Vostok ice core: a continuous isotope temperature record over the last climatic cycle (160,000 years). *Nature 329*, 403–408.

Levitus, S. 1982. Atlas of the World Ocean. *NOAA Professional Paper*, 13, Rockville Md.

Lorius, C., Jouzel, J., Ritz, C., Merlivat, L., Barkov, N. I., Korotkevich, Y. S. and Kotlyakov, V. M. 1985. A 150,000-year climatic record from Antarctic ice. *Nature 316*, 591–596.

Maier-Reimer, E. and Hasselmann, K. 1987. Transport and storage of CO_2 in the ocean. An inorganic ocean-circulation carbon cycle model. *Climate Dynamics 2*, 63–90.

Maier-Reimer, E. and Mikolajewicz, U. 1989. Experiments with an OGCM on the cause of the Younger Dryas. pp. 87–100. In: *Oceanography 1988.* (eds. A. Ayala-Castañares, W., Wooster, and A. Yañez-Arancibia), UNAM Press, México D F, 208 pp.

Manabe, S. and Stouffer, R. J. 1988. Two stable equilibria of a coupled ocean-atmosphere model. *J. Climate 1*, 841–866.

Marotzke, J., Welander, P. and Willebrand, J. 1988. Instability and multiple steady states in a meridional-plane model of the thermohaline circulation. *Tellus 40A*, 162–172.

Mikolajewicz, U. 1990. *Interne Variabilität in einem stochastisch angetriebenen ozeanischen Zirkulationsmodell.* Ph.D. Thesis, Univ. Hamburg, 125 pp. (In German)

Mikolajewicz, U. and Maier-Reimer, E. 1990. Internal secular variability in an ocean general circulation model. *Climate Dynamics. 4*, 145–156.

Mitchell, J. M. Jr. 1966. Stochastic models of air-sea interaction and climatic fluctuation. *Symp. on the Arctic Heat Budget and Atmospheric Circulation*, Lake Arrowhead, Calif., The Rand Corp., Santa Monica, Research Memorandum RM-5233-NSF, 45–74.

Oberhuber, J. M. 1990. Simulation of the Atlantic circulation with a coupled sea ice-mixed layer-isopycnal general circulation model. Max-Planck-Institut für Meteorologie, Hamburg, Germany, Report No. 59, 86 pp.

Roeckner, E., Dümenil, L., Kirk, E., Lunkeit, F., Ponater, M., Rockel, B., Sausen, R. and Schlese, U. 1989. The Hamburg version of the ECMWF model (ECHAM). In G. J. Boer: *Research activities in atmosphere and oceanic modelling*, CAS/JSC Working Group on Numerical Experimentation, Report No. 12, WMO/TD-332, 7.1–7.4.

Romeiser, R. 1991. Validation of the WAM wave prediction model by GEOSAT wave hight data. Zentrum für Meeres- und Klimaforschung, Hamburg, Germany, Report No. 13.

Sarmiento, J. L. and Bryan, K. 1982. An ocean transport model for the North Atlantic. *J. Geophys. Res. 87*, 394–408.

Sausen, R., Barthel, K. and Hasselmann, K. 1988. Coupled ocean-atmosphere models with flux correction. *Climate Dynamics 2*, 145–163.

Stigebrandt, A. 1985. On the hydrographic and ice conditions in the northern North Atlantic during different phases of a glaciation cycle. *Palaeogeogr. Palaeoclimatol. Palaeoecol. 50*, 303–321.

Stouffer, R. J., Manabe, S. and Bryan, K. 1989. Interhemispheric asymmetry in climate response to a gradual increase of atmospheric CO_2. *Nature 342*, 660–662.

Toggweiler, J. R., Dixon, K. and Bryan, K. 1989a. Simulations of Radiocarbon in a Coarse-Resolution World Ocean Model, 1. Steady State Prebomb Distributions. *J. Geophys. Res. 94, C6*, 8217–8242.

Toggweiler, J. R., Dixon, K. and Bryan, K. 1989b. Simulations of Radiocarbon in a Coarse-Resolution World Ocean Model, 2. Distributions of Bomb-Produced Carbon 14. *J. Geophys. Res. 94, C6*, 8243–8264.

WAMDIG (WAM-Development and Implementation Group): Hasselmann, S., Hasselmann, K., Bauer, E., Jansen, P. A. E. M., Komen, G. J., Bertotti, L., Lionello, P., Guillaume, A., Cardone, C. V., Greenwood, J. A., Reistad, M., Zambresky, L. and Ewing, J. A. 1988. The WAM Model. A third generation ocean wave prediction model. *J. Phys. Oceanogr. 18*, 1775–1810.

Washington, W. M. and Meehl, G. A. 1989. Climate sensitivity due to increased CO_2: Experiments with a coupled atmosphere and ocean general circulation model. *Climate Dynamics 4*, 1–38.

Welander, P. 1986. Thermohaline effects in the ocean circulation and related simple models. In: *Large-scale transport processes in oceans and atmosphere*. (eds. J. Willebrand and D. L. T. Anderson). Reidel, Dordrecht, 163–200.